

# Computational Investigations of the Primary Excited States of Poly(*para*-phenylene vinylene)

Robert J. Bursill<sup>1</sup> and William Barford<sup>2</sup>

<sup>1</sup>*School of Physics, University of New South Wales, Sydney, New South Wales 2052, Australia*

<sup>2</sup>*Department of Physics and Astronomy, University of Sheffield, Sheffield, S3 7RH, United Kingdom*

The Pariser-Parr-Pople model of  $\pi$ -conjugated electrons is solved by the density matrix renormalization group method for the light emitting polymer, poly(*para*-phenylene vinylene). The energies of the primary excited states are calculated. When solid state screening is incorporated into the model parameters there is excellent agreement between theory and experiment, enabling an identification of the origin of the key spectroscopic features.

PACS numbers: 71.10.-w, 71.20.Rv, 71.35.-y, 78.67.-n

## I. INTRODUCTION

Since the discovery of electroluminescence in poly(*para*-phenylene vinylene) (PPV) in 1990<sup>1</sup>, a variety of experimental and theoretical techniques have been deployed to investigate the physics of the primary photoexcitations of the phenyl-based light emitting polymers. Linear and non-linear optical spectroscopies have revealed the energies and symmetries of the dominant dipole-allowed transitions, as well as the important dipole-forbidden transitions that participate in non-linear optical processes.

All phenyl-based light emitting polymers exhibit a characteristic absorption spectra. These show two dominant excitations polarized parallel to the chain axis (at 2.8 eV and 6.1 eV in PPV<sup>2</sup>). There are also two intermediate weaker transitions (at 3.6 eV and 4.8 eV in PPV<sup>2</sup>). The higher of these intermediate transitions is predominantly polarized perpendicular to the chain axis, whereas the polarization of the lower transition is less well-defined. (In PPV it is predominately polarized parallel to the long-axis<sup>3</sup>.) Furthermore, the strength of this lower transition is enhanced by chemical substitution. Electroabsorption<sup>2</sup> and two-photon absorption<sup>4</sup> reveal a dipole-forbidden state at approximately 0.7 eV above the lowest dipole-allowed transition. These two states are usually labelled the  $m^1A_g$  and  $1^1B_u$  states, respectively. Finally, a triplet state has been observed at 0.7 eV below the  $1^1B_u$  excitation (see ref<sup>5</sup> for references), with another dipole connected triplet state 1.4 eV higher in energy<sup>6</sup>. (Notice that this higher triplet state, labelled as the  $m^3A_g$  state, is virtually degenerate with its singlet counterpart, namely the  $m^1A_g$  state. These two states are often referred to as the singlet and triplet charge-transfer states. Their degeneracy can be explained by the fact that they are the lowest pseudomomentum branches of the  $n = 2$  Mott-Wannier excitons, which have odd parity electron-hole wavefunctions and therefore experience no exchange interactions<sup>7</sup>.)

An important early insight into the nature of the primary photoexcitations of the phenyl-based systems was provided by Rice and Gartstein<sup>8,9</sup>, who argued that they can essentially be understood as arising from the delocal-

ization of the primitive benzene excitations. Kirova and Brazovskii, on the other hand, have argued that a conventional semiconductor band picture of bound particle-hole excitations is a more appropriate description<sup>10</sup>. Other theoretical work on PPV includes, a single configuration interaction (CI) calculation of the Pariser-Parr-Pople model by Chandross and Mazumdar<sup>11</sup>; density matrix renormalization group calculations on reduced molecular-orbital models by Barford *et al.*<sup>12</sup>; quantum chemistry calculations on the INDO Hamiltonian by Beljonne *et al.*<sup>13</sup>, and Weibel and Yaron<sup>14</sup>; and *ab initio* Bethe-Salpeter equation (BSE) calculations by Rohlfiing and Louie<sup>15</sup>. These theoretical predictions will be discussed more fully in Section III, when we discuss the results of the calculations presented here and their comparisons to experiment.

In this paper we present density matrix renormalization group (DMRG) calculations on the full Pariser-Parr-Pople model of PPV. The DMRG method for calculating the full electronic spectra of conjugated polymers has a number of advantages over its competitors. It is more accurate than single or double CI calculations, and does not suffer from finite-size consistency errors; it makes no assumptions about the nature of the excitations (unlike the BSE method, which assumes that the excitations are particle-hole pairs), thus it is able to accurately model highly correlated excited states; and unlike standard quantum chemistry techniques, it is able to calculate the excited spectra of large molecules. The DMRG method is most readily suited to reduced basis Hamiltonians, such as the  $\pi$ -electron Pariser-Parr-Pople model. This is not necessarily a disadvantage over *ab initio* methods, as when correctly parameterized the Pariser-Parr-Pople model makes very accurate predictions<sup>11,16</sup>. Moreover, the Pariser-Parr-Pople model possess particle-hole symmetry, which means that spatial, particle-hole and spin-flip symmetries can be employed to target high-lying excited states in the DMRG method (see ref<sup>17</sup>, for example).

DMRG calculations on the full Pariser-Parr-Pople model were presented for poly(*para*-phenylene) by Bursill and Barford<sup>18</sup>. This paper extends that approach to PPV. In the next section we define the Pariser-Parr-

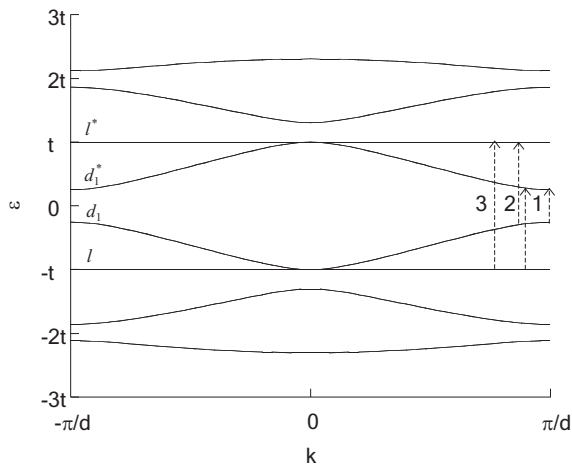


FIG. 1: The band structure of PPV with all nearest neighbor bond integrals,  $t$ , equal. The low-lying particle-hole transitions are labelled 1, 2 and 3.

Pople model and briefly describe our implementation of the DMRG method. In Section III we describe and discuss our results, and compare them to other approaches, concluding in section IV.

## II. MODEL AND METHODOLOGY

### A. The Pariser-Parr-Pople Model

The Pariser-Parr-Pople model is a  $\pi$ -electron model of conjugated polymers, defined by,

$$\begin{aligned} \mathcal{H} = & - \sum_{\langle ij \rangle \sigma} t_{ij} \left[ c_{i\sigma}^\dagger c_{j\sigma} + c_{j\sigma}^\dagger c_{i\sigma} \right] \\ & + U \sum_i (n_{i\uparrow} - 1/2)(n_{i\downarrow} - 1/2) \\ & + \frac{1}{2} \sum_{i \neq j} V_{ij} (n_i - 1)(n_j - 1), \end{aligned} \quad (1)$$

where  $\langle \rangle$  represents nearest neighbors,  $c_{i\sigma}$  destroys a  $\pi$ -electron on site  $i$ ,  $n_{i\sigma} = c_{i\sigma}^\dagger c_{i\sigma}$ , and  $n_i = n_{i\uparrow} + n_{i\downarrow}$ .

We use the Ohno parameterization for the Coulomb interaction, defined by,

$$V_{ij} = U / \sqrt{1 + (U\epsilon r_{ij}/14.397)^2}, \quad (2)$$

where  $r_{ij}$  is the inter-atomic distance (in Å),  $U$  is the on-site Coulomb interaction (in eV), and  $\epsilon$  is the dielectric constant. This interaction is an interpolation between an on-site Coulomb repulsion,  $U$ , and a Coulomb potential,  $e^2/4\pi\epsilon_0 r_{ij}$  as  $r_{ij} \rightarrow \infty$ .

The band structure, obtained in the non-interacting limit ( $U = 0$ ), is shown in Fig. 1. The pair of non-bonding bands are a consequence of the  $D_{2h}$  symmetry

of the Hamiltonian in the non-interacting limit with only nearest-neighbor bond integrals. The low-lying particle-hole excitations are labelled 1 (for transitions involving  $d_1$  and  $d_1^*$ ), the degenerate pair labelled 2 (for transitions involving  $d_1$  and  $l^*$ , and  $l$  and  $d_1^*$ ), and 3 (for transitions involving  $l$  and  $l^*$ ). Coulomb interactions lift the degeneracy of the intermediate pair (which become the intermediate pair of transitions described in Section I), while the transitions 1 and 3 become the low and high energy transitions described in Section I. Evidently, to obtain a more realistic description of the excited states it is necessary to include Coulomb interactions.

In the following we use two sets of parameters to model the excited states. The first set, called the *optimized* parameters, were derived by fitting the predicted Pariser-Parr-Pople excitation energies of stilbene to the experimental spectrum of stilbene in vacuo<sup>19</sup>. These are,  $t_p = 2.539$  eV,  $t_d = 2.684$  eV,  $t_s = 2.22$  eV,  $U = 10.06$  eV, and  $\epsilon = 1$  (where the phenyl, double and single bond integrals are defined in Fig. 2). Although giving instructive results, this parameter set fails to quantitatively predict the excitation energies of polymers in the solid state, as they fail to account for the solvation effects of the surrounding dielectric<sup>20,21</sup>. The other parameter set, called the *screened* parameters, were derived by Chandross and Mazumdar<sup>11</sup> to account for solid state solvation effects. These parameters are,  $t_p = 2.4$  eV,  $t_d = 2.6$  eV,  $t_s = 2.2$  eV,  $U = 8$  eV, and  $\epsilon = 2$ .

### B. The Density Matrix Renormalization Group (DMRG) Method

Eq. (1) is solved by the DMRG method for chains of up to 28 phenyl rings (i.e. 222 sites). The DMRG method is an efficient truncation procedure for solving quantum lattice Hamiltonians, especially in one-dimension<sup>22</sup>. The details of the DMRG implementation for this problem, particularly the procedure of deriving an optimized reduced basis for the phenyl ring<sup>18,23,24</sup>, are described in detail in ref<sup>18</sup>. Also shown in ref<sup>18</sup> are comprehensive DMRG convergence tests that are applicable to phenyl-based systems.

As described in Section I, the Pariser-Parr-Pople model possess spin-flip and particle-hole symmetries, which we exploit in the DMRG method to target excited states. With only onsite and nearest neighbor Coulomb interactions the Pariser-Parr-Pople model applied to the PPV structure formally possess  $D_{2h}$  symmetry. In this limit this means that the eigenstates are labelled with the spatial symmetry assignments,  $A_g$ ,  $B_{1u}$ ,  $B_{2u}$ , and  $B_{3g}$ . Longer range Coulomb interactions with the PPV structure reduce the  $D_{2h}$  symmetry to  $C_2$  symmetry, and thus the true spatial symmetry assignments are  $A_g$  and  $B_u$ . However, it is computationally expedient, with very little loss of accuracy, to retain  $D_{2h}$  symmetry while incorporating long range Coulomb interactions. This is achieved by taking the bond angle between the single and double

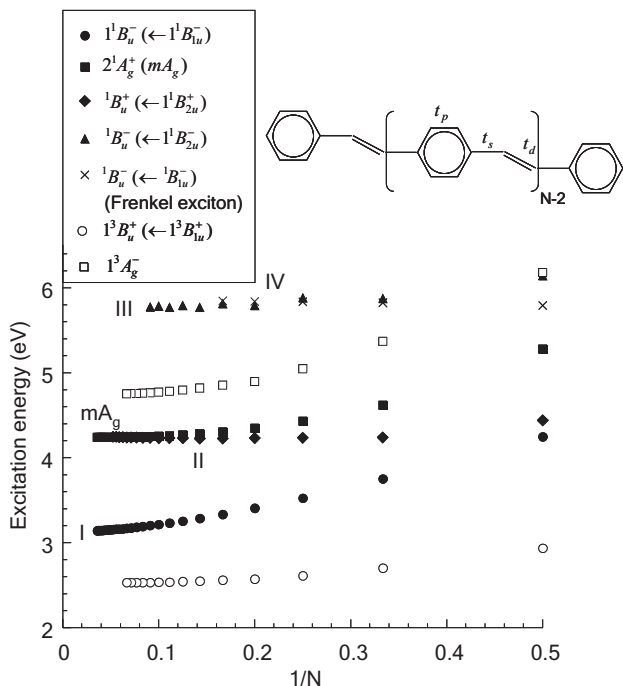


FIG. 2: The DMRG calculated transition energies of *para*-phenylene vinylene oligomers as a function of inverse chain length, calculated from the Pariser-Parr-Pople model with optimized parameters:  $U = 10.06$  eV,  $t_p = 2.539$  eV,  $t_d = 2.684$  eV,  $t_s = 2.22$  eV, and dielectric constant,  $\epsilon = 1$ . The excited states are identified with the spectroscopic features shown in Fig. 3 of ref<sup>2</sup> and Fig. 1 of ref<sup>4</sup>. The symmetry assignments of the states shown in brackets are the symmetries the eigenstates would have if PPV had  $D_{2h}$  rather than  $C_2$  symmetry. The inset shows the oligo-phenylene vinylene structure with the bond integrals  $t_p$ ,  $t_d$  and  $t_s$ .

bonds in the vinyne unit to be  $180^\circ$ , rather than  $120^\circ$ . To ensure that the overall molecular size is consistent to the original structure the single and double lengths are reduced to  $1.283 \text{ \AA}$  and  $1.194 \text{ \AA}$ , respectively. The phenyl bond length is  $1.40 \text{ \AA}$ . The next section describes the calculated results.

### III. RESULTS AND DISCUSSIONS

#### A. DMRG Calculations

Fig. 2 shows the DMRG calculated excitation energies of oligo(*para*-phenylene vinylenes) using the Pariser-Parr-Pople model with unscreened parameters ( $U = 10.06$  eV,  $t_p = 2.539$  eV,  $t_d = 2.684$  eV,  $t_s = 2.22$  eV, and  $\epsilon = 1$ ). ( $N = 2$  corresponds to stilbene.) The  $1^1B_u^-$  state is the strong lowest energy dipole allowed transition (labelled I in Fig. 3 of ref<sup>2</sup>). The strong transition dipole moment between this state and the  $2^1A_g^+$  state indicates that the  $2^1A_g^+$  is the state labelled ‘ $m^1A_g$ ’ in non-linear

optical spectroscopies (see, for example, Fig. 1(a) in ref<sup>4</sup>). The energies of the  $1^1B_u^-$  and  $2^1A_g^+$  states initially reduce rapidly as a function of chain length, indicating that these states reduce their kinetic energy by readily delocalizing the exciton wavefunction along the chain. This is primarily because these states are largely constructed from particle-hole transitions between the bonding and antibonding bands, labelled  $d_1$  and  $d_1^*$  in Fig. 12<sup>5</sup>. A description of these states as strongly bound band exciton states is therefore appropriate in the long-chain limit. Indeed, the  $1^1B_u^-$  state is the lowest pseudomomentum branch of the  $n = 1$  Mott-Wannier exciton, while the  $2^1A_g^+$  is the lowest pseudomomentum branch of the  $n = 2$  Mott-Wannier exciton<sup>7,17</sup>. (Higher lying pseudo-momentum branches of the  $n = 1$  and  $n = 2$  excitons for DMRG calculations on poly(*para*-phenylene) are illustrated in Fig. 5 of ref<sup>18</sup>.) Notice that this assignment places a *lower bound* on the binding energy of the  $n = 1$  exciton as  $E(mA_g) - E(1B_u)$ .

We next consider the state labelled II and shown by diamonds in Fig. 2. This state has  $1^1B_u^+$  symmetry, but would have  $1^1B_{2u}^+$  symmetry if PPV had  $D_{2h}$  symmetry. From a band picture analysis, this state is composed of an antisymmetric combination of particle-hole transitions from  $d_1$  to  $l^*$  and  $l$  to  $d_1^*$ . At the Pariser-Parr-Pople model level, it has positive particle-hole symmetry, and is therefore dipole-forbidden. However, it is weakly dipole allowed in real systems, and its oscillator strength is further enhanced by chemical substitution. Its excitation energy is virtually independent of chain length, because, first its wavefunction is composed of non-bonding orbitals, and therefore there is no hybridization via one-electron transfer terms, and second since it has a very small oscillator strength, resonant exciton transfer along the chain is virtually inoperative. These two features (weak oscillator strength and a chain independent energy) strongly indicate that the second spectroscopic feature (labelled II in Fig. 3 of ref<sup>2</sup>) originates from this state.

The state labelled III and shown by triangles in Fig. 2 has  $1^1B_u^-$  symmetry, but would have  $1^1B_{2u}^-$  symmetry if PPV had  $D_{2h}$  symmetry. From a band picture analysis, this state is composed of a symmetric combination of particle-hole transitions from  $d_1$  to  $l^*$  and  $l$  to  $d_1^*$ . It has negative particle-hole symmetry, and therefore has an allowed dipole transition from the ground state. This state is the third spectroscopic feature of PPV (labelled III in Fig. 3 of ref<sup>2</sup>).

The state labelled IV and shown by crosses in Fig. 2 has  $1^1B_u^-$  symmetry, but would have  $1^1B_{1u}^-$  symmetry if PPV had  $D_{2h}$  symmetry. From a band picture analysis, this state is composed of particle-hole transitions from  $l$  to  $l^*$ . It has negative particle-hole symmetry, has a strong dipole transition from the ground state, and is polarized along the chain axis. This state is the fourth spectroscopic feature of PPV (labelled IV in Fig. 3 of ref<sup>2</sup>), as is usually referred to as the ‘Frenkel’ exciton, as its particle-hole wavefunction is typically confined to a single phenyl-ring.

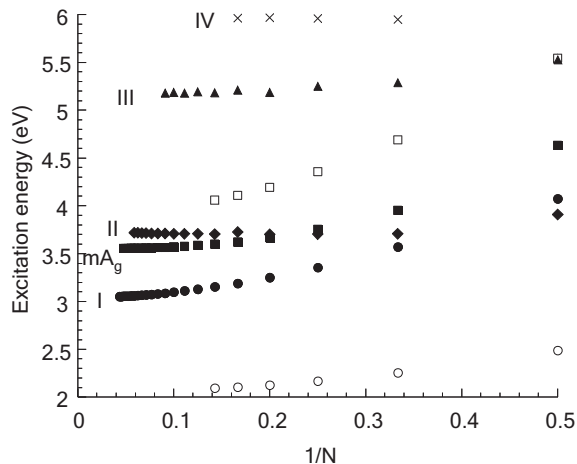


FIG. 3: The DMRG calculated transition energies of *para*-phenylene vinylene oligomers as a function of inverse chain length, calculated from the Pariser-Parr-Pople model with screened parameters:  $U = 8$  eV,  $t_p = 2.4$  eV,  $t_d = 2.6$  eV,  $t_s = 2.2$  eV, and  $\epsilon = 2$ . The symbols are defined in the inset of Fig. 2. The excited states are identified with the spectroscopic features shown in Fig. 3 of ref<sup>2</sup> and Fig. 1 of ref<sup>4</sup>.

Finally, the two triplet states,  $1^3B_u^+$  and  $m^3A_g^-$ , are also shown in Fig. 2.

The results shown in Fig. 2 are obtained from the Pariser-Parr-Pople model with optimized parameters that are not parametrized to model solid state solvation effects. The dielectric response of the environment is predicted to red-shift the intra-molecular excitations of a single chain by up to 0.1 eV for the  $1^1B_u$  state, 0.7 eV for the  $m^1A_g$  state, and 1.5 eV for the charge gap<sup>20,21</sup>. We would therefore not expect these calculations on a single chain to compare directly with experimental observations.

Chandross and Mazumdar attempted to model solvation effects by adjusting the Pariser-Parr-Pople parameters and introducing a static dielectric constant<sup>11</sup>. Although the introduction of a *static* dielectric constant is not a faithful representation of the dielectric response (because the timescale for the particle-hole motion is very similar to the timescale of the dielectric response<sup>20</sup>), these screened parameters do lead to Pariser-Parr-Pople model predictions that are remarkably close to the experimental observations.

Fig. 3 shows the DMRG calculated results with the screened parameters ( $U = 8$  eV,  $t_p = 2.4$  eV,  $t_d = 2.6$  eV,  $t_s = 2.2$  eV, and  $\epsilon = 2$ ). Comparing this figure with Fig. 2 we see that the  $1^1B_u^-$  and  $2^1A_g^+$  states are red-shifted by ca. 0.1 eV and 0.6 eV, respectively, as expected from solvation effects. The excited states are identified with the spectroscopic features shown in Fig. 3 of ref<sup>2</sup>. Their energies are remarkably consistent with the experimental values of 2.8, 3.6, 4.8, and 6.1 eV obtained in ref<sup>2</sup>, lending additional credence to our assignments of the excited

state origins of the features, discussed above.

## B. Other Approaches

We now compare our DMRG predictions of the Pariser-Par-Pople model with other approaches. Our results using the screened parameters are consistent with those of Chandross and Mazumdar<sup>11</sup>. They used SCI on the Pariser-Par-Pople model. For an eight-unit oligomer they calculate the  $1^1B_u$  state at 2.7 eV, an  $m^1A_g$  state at 3.3 eV, and the  $n^1B_u$  state at 3.6 eV. The  $1^1B_u$  and  $m^1A_g$  states are the  $n = 1$  and  $n = 2$  excitons, while the  $n^1B_u$  state coincides with the charge-gap and therefore indicates the onset of the particle-hole continuum. They also predict the  $1^3B_u$  state at 1.4 eV.

An *ab initio* BSE calculation by Rohlfing and Louie<sup>15</sup> on a PPV polymer predicts dipole allowed and forbidden singlet excitons at 2.4 eV and 2.8 eV, respectively, with the quasi-particle gap at 3.3 eV. They also predict triplet excitons at 1.5 eV and 2.7 eV. The 2.4 eV and 2.8 eV singlet excitons are the  $1^1B_u$  and  $m^1A_g$  states, respectively, while the 1.5 eV and 2.7 eV triplet excitons are the  $1^3B_u$  and  $m^3A_g$  states, respectively. The  $m^1A_g$  and  $m^3A_g$  states are nearly degenerate, as predicted by the Mott-Wannier exciton theory for odd parity particle-hole wavefunctions. Using the same technique with a screened electron-hole interaction van der Horst *et al.*<sup>26</sup> predict a  $1^1B_u$  binding energy in PPV of 0.48 eV.

The origin of the higher-lying transitions has also been investigated. Rohlfing and Louie<sup>15</sup>, and Weibel and Yaron<sup>14</sup> predict that peak II in PPV arises from an exciton caused predominately by the antisymmetric combination of particle-hole transitions from  $d_1$  to  $l^*$  and  $l$  to  $d_1^*$ . Weibel and Yaron<sup>14</sup> have also investigated the effects of breaking particle-hole symmetry on the oscillator strength and polarization of peak II. Using the semiempirical INDO Hamiltonian on nonplanar dihydroxy-PPV, their calculations indicate that chemical substitution and mixing of the  $\pi$  and  $\sigma$  orbitals enhances the oscillator strength, as originally suggested by Gartstein *et al.*<sup>9</sup> Moreover, as illustrated in Fig. 5 of ref<sup>14</sup>, this peak becomes predominately polarized along the chain axis, in agreement with experiment<sup>3</sup>.

## IV. CONCLUSIONS

Gathering together the various theoretical predictions of the origins of the primary excited states of PPV we now interpret the key spectroscopic features of PPV.

Peak I corresponds to the low-energy dipole active  $1^1B_u^-$  state. This is the lowest pseudomomentum branch of the family of  $n = 1$  Mott-Wannier singlet excitons resulting from the Coulomb attraction between the particle-hole excitation from the valence ( $d_1$ ) to the conduction ( $d_1^*$ ) bands. Approximately 0.7 eV higher in energy is the  $m^1A_g$  state, identified by electroabsorption<sup>2</sup>,

two-photon absorption and photoinduced absorption<sup>4</sup>. The Pariser-Parr-Pople model calculations described in this paper suggest that this state is the  $2^1A_g^+$  state, which is the lowest pseudomomentum branch of the family of  $n = 2$  Mott-Wannier excitons. This assignment places a lower bound on the spectroscopically determined binding energy of the  $1^1B_u$  exciton of 0.7 eV. Approximately 0.7 eV below the  $1^1B_u^-$  exciton is the  $1^3B_u^+$  triplet, indicating a large exchange energy characteristic of correlated states. This state is the lowest pseudomomentum branch of the family of  $n = 1$  Mott-Wannier triplet excitons. Photo-induced absorption from the  $1^3B_u^+$  triplet indicates another triplet, the  $1^3A_g^-$  state, at approximately 1.4 eV higher in energy, and essentially degenerate with the  $2^1A_g^+$  state. This triplet state is the lowest pseudomomentum branch of the family of  $n = 2$  Mott-Wannier triplet excitons. As expected from Mott-Wannier exciton theory in one-dimension<sup>7,17</sup>, the odd particle-hole parity singlet and triplet (charge-transfer) excitons are virtually degenerate. The  $n^1B_u$  state at 0.1 eV higher in energy than the  $m^1A_g$  state in PPV<sup>2</sup> indicates binding energies of  $\sim 0.8$  eV and 0.1 eV for the  $n = 1$  and  $n = 2$  singlet excitons, respectively. Higher in energy are the excita-

tions associated with peaks II and III. These arise from antisymmetric and symmetric combinations of particle-hole transitions from  $d_1$  to  $l^*$  and  $l$  to  $d_1^*$ , respectively. Finally, peak IV is the intraphenyl, or Frenkel, exciton. This identification of the primary excited states of PPV also applies to other phenyl-based systems, e.g. PPP<sup>17,18</sup>.

The calculations presented in this paper have entirely concerned vertical transitions, where the excited states are calculated in the geometry of the ground state. Of course, electron-lattice relaxation is an important process in polymers that determines Stokes shifts, self-trapping, and exciton and charge transfer between polymers. The consequences of electron-lattice relaxation on the excited states energies and structures have been considered in refs<sup>27</sup>.

### Acknowledgments

R. J. B. acknowledges support from the Australian Research Council and the J. G. Russell Foundation. W. B. thanks the Leverhulme Trust for financial support.

- 
- E.mail addresses: ph1rb@phys.unsw.edu.au,  
W.Barford@sheffield.ac.uk
- <sup>1</sup> J. H. Burroughes, D. D. C. Bradley, A. R. Brown, R. N. Marks, K. Mackay, R. H. Friend, P. L. Burn, and A. D. Holmes, *Nature* **347**, 539 (1990)
  - <sup>2</sup> S. J. Martin, D. D. C. Bradley, P. A. Lane, H. Mellor, and P. L. Burn, *Phys. Rev. B* **59**, 15133 (1999)
  - <sup>3</sup> E. K. Miller, D. Yoshida, C. Y. Yang, and A. J. Heeger, *Phys. Rev. B* **59**, 4661 (1999)
  - <sup>4</sup> S. Frolov, Z. Bao, M. Wohlgenannt, and Z. V. Vardeny, *Phys. Rev. B* **65**, 205209 (2002)
  - <sup>5</sup> A. Köhler and D. Beljonne, *Advanced Functional Materials* **14**, 11 (2004)
  - <sup>6</sup> A. P. Monkman, H. D. Burrows, L. J. Hartwell, L. E. Horsburgh, I. Hamblett, and S. Navaratnam, *Phys. Rev. Lett.* **86**, 1358 (2001)
  - <sup>7</sup> W. Barford, R. J. Bursill, and R. W. Smith, *Phys. Rev. B* **66**, 115205 (2002)
  - <sup>8</sup> M. J. Rice and Yu. N. Gartstein, *Phys. Rev. Lett.* **73**, 2504 (1994)
  - <sup>9</sup> Yu. N. Gartstein, M. J. Rice, and E. M. Conwell, *Phys. Rev. B* **52**, 1683 (1995)
  - <sup>10</sup> N. Kirova, S. Brazovskii, and A. R. Bishop, *Synth. Metals* **100**, 29 (1999); N. Kirova and S. Brazovskii, *Synth. Metals* **141**, 139 (2004)
  - <sup>11</sup> M. Chandross and S. Mazumdar, *Phys. Rev. B* **55**, 1497 (1997)
  - <sup>12</sup> W. Barford and R. J. Bursill, *Chem. Phys. Lett.*, **268**, 535 (1997); M. Lavrentiev, W. Barford, S. Martin, H. Daly, and R. J. Bursill, *Phys. Rev. B* **59**, 9987 (1999); R. J. Bursill, W. Barford, and H. Daly, *Chem. Phys.*, 243, 35 (1999)
  - <sup>13</sup> D. Beljonne, Z. Shuai, J. Cornil, D. A. dos Santos, and J. L. Brédas, *J. Chem. Phys.* **111**, 2829 (1999)
  - <sup>14</sup> J. D. Weibel and D. Yaron, *J. Chem. Phys.* **116**, 6846 (2002)
  - <sup>15</sup> M. Rohlfing and S. G. Louie, *Phys. Rev. Lett.* **82**, 1959 (1999)
  - <sup>16</sup> R. J. Bursill, C. Castleton, and W. Barford, *Chem. Phys. Lett.* **294**, 305 (1998)
  - <sup>17</sup> W. Barford, *Electronic and Optical Properties of Conjugated Polymers*, Oxford University Press, Oxford (2005)
  - <sup>18</sup> R. J. Bursill and W. Barford, *Phys. Rev. B* **66**, 205112 (2002)
  - <sup>19</sup> C. Castleton and W. Barford, *Synth. Met.* **101**, 520 (1999); C. W. M. Castleton and W. Barford, *J. Chem. Phys.*, **117**, 3570 (2002)
  - <sup>20</sup> E. Moore, B. Gherman, and D. Yaron, *J. Chem. Phys.* **106** 4216 (1997); E. Moore and D. Yaron, *J. Chem. Phys.* **109**, 6147 (1998)
  - <sup>21</sup> W. Barford, R. J. Bursill, and D. Yaron, *Phys. Rev. B* **69**, 155203 (2004)
  - <sup>22</sup> S. R. White, *Phys. Rev. Lett.* **69**, 2863 (1992)
  - <sup>23</sup> C. Zhang, E. Jeckelmann, and S. R. White, *Phys. Rev. Lett.* **80** 2661 (1998)
  - <sup>24</sup> W. Barford, R. J. Bursill, and M. Lavrentiev, *Phys. Rev. B* **65**, 075107 (2002); W. Barford and R. J. Bursill, *Phys. Rev. B* (in press)
  - <sup>25</sup> However, as the chain length decreases below the particle-hole separation there is also a ‘quantum confinement’ effect, arising from the squeezing of the particle-hole wavefunction. See, for example, Z. Shuai, J. L. Bredas, S. K. Pati, and S. Ramasesha, *Phys. Rev. B* **56**, 9298 (1997); M. Y. Lavrentiev and W. Barford, *Phys. Rev. B* **59**, 15 048 (1999)
  - <sup>26</sup> J-W. van der Horst, P. A. Bobbert, M. A. J. Michels, and H. Bässler, *J. Chem. Phys.* **114**, 6950 (2001)
  - <sup>27</sup> C. Ambrosch-Draxl, J. A. Majewski, P. Vogl, and G. Leis-

ing, *Phys. Rev. B* **51**, 9668 (1995); D. Beljonne, Z. Shuai, R. H. Friend, and J. L. Brédas, *J. Chem. Phys.* **102**, 2042 (1995); E. Zojer, N. Koch, P. Puschnig, F. Meghdadi, A. Niko, R. Resel, C. Ambrosch-Draxl, M. Knupfer, J. Fink, J. L. Brédas, and G. Leising, *Phys. Rev. B* **61**, 16538 (2000); S. Tretiak, A. Saxena, R. L. Martin, and A. R.

Bishop, *Phys. Rev. Lett.*, **89**, 097402 (2002); E. Artacho, M. Rohlfing, M. Côte, P. D. Haynes, R. J. Needs, and C. Molteni, *Phys. Rev. Lett.* **93**, 116401 (2004); E. Moore, W. Barford, and R. J. Bursill, *Phys. Rev. B* **71**, 115107 (2005)